Natural zeolite as a supporting material of TiO2 and ZnO photocatalysts for UV-induced Congo red photodegradation

Natural zeolite as a supporting material of TiO_2 and ZnO photocatalysts for UV-induced Congo red photodegradation

L H Ulya[1*], A N Faiza[1], M F Maulani[1], Kustomo[2,3] and Kholidah[2]

[1] Laboratory of Inorganic Chemistry, Department of Chemistry, Faculty of Science and Technology, Universitas Islam Negeri Maulana Malik Ibrahim Malang, Malang, Indonesia
[2] Chemistry Study Program, Faculty of Science and Technology, Universitas Islam Negeri Walisongo, Semarang, Indonesia
[3] Department of Chemistry, Faculty of Science, National University of Singapore, 3 Science Drive 3, Lower Kent Ridge, Singapore

[*]*E-mail: luluhamida@uin-malang.ac.id

Abstract. Congo red dye (CRD) is highly toxic and can harm aquatic organisms. Photodegradation is an alternative solution that can be used to treat dyes. TiO_2 and ZnO are semiconductor materials commonly utilised in photocatalysts due to their photocatalytic activity. Yet, both TiO_2 and ZnO have a small surface area; hence, their performance is inadequate when employed in their bare state. The photocatalytic activity of TiO_2 and ZnO can be enhanced by depositing them on the zeolite. Both were attached to natural zeolite using the sonication method, and the photocatalytic activity was examined with variation in irradiation time, photocatalyst mass, and dye concentration. The XRD results show that TiO_2-natural zeolite (TNZ) and ZnO-natural zeolite (ZNZ) contain an anatase phase of TiO_2, a wurtzite phase of ZnO and mordenite zeolite. Then, the results of the FTIR spectra of TNZ and ZNZ showed that TiO_2 and ZnO were successfully embedded on the surface of the natural zeolite (NZ). The optimum time obtained in the CRD photodegradation process was 100 minutes, and the optimum concentration of CRD degradation was 10 ppm for TNZ and 15 ppm for ZNZ photocatalysts. Interestingly, the optimum mass of TNZ and ZNZ photocatalyst was 30 and 200 mg, respectively.

Keyword : TiO_2, ZnO, photocatalyst, photodegradation, Congo red

1. Introduction

According to a 2021 estimate from the National Development Agency of Indonesia, the Indonesian textile sector is predicted to generate 3.9 million tonnes of textile waste by 2030 [1]. The textile sector is considered to be responsible for approximately 20% of global clean water contamination through dyeing and finishing operations [2]. One of dyes that usually used is Congo red dye (CRD), The CRD is known to be carcinogenic because of the presence of aromatic amine groups [3]. The complex aromatic structure of CRD contributes to its hazardous qualities, making it a focus of concern in environmental health studies [3]. On the other hand, studies have shown that CRD has

a considerable impact on the survival and reproduction of aquatic species such as *Ceriodaphnia dubia*, with deadly doses as low as 3 mg/L. Sublethal exposure resulted in lower survival rates and fertility, emphasizing the environmental dangers of CRD discharge into water bodies [4].

Several approaches, including TiO_2-based photocatalysis, have been investigated for CRD degradation, with degradation efficiency achieved under ideal conditions [5]. Titanium dioxide (TiO_2) is an efficient semiconductor photocatalyst for degrading organic contaminants in wastewater, with excellent stability, low cost, and nontoxicity [6]. The use of it as a semiconductor photocatalyst for wastewater treatment has received a lot of attention because of its ability to degrade organic contaminants. TiO_2 works by producing reactive species under UV radiation, which aids in the degradation of pollutants into harmless by products. When exposed to UV radiation, TiO_2 produces hydroxyl radicals from adsorbed molecular oxygen, oxidizing organic pollutants in water [7]. TiO_2 has been effectively utilized to remediate contaminated river water, with up to 98% breakdown of organic pollutants [8].

On the other hand, ZnO NPs exhibit excellent photocatalytic activity for degrading CRD, demonstrating their potential for processing liquid waste in the textile industry [9] [10]. Similar to TiO_2, ZnO has also been effectively used in various studies for degrading pollutants in car wash wastewater and textile effluents, achieving degradation efficiencies of up to 98.9% for specific dyes [11]. ZnO serves as a superior photocatalyst for photodegradation due to its affordability, eco-friendliness, and ability to fully mineralize pollutants [12].

However, TiO_2 and ZnO are difficult to separate and recover from reaction medium [13], tend to agglomerate due to their high surface energy [14], and suffer from rapid recombination of photogenerated electron-hole pairs, which limits their quantum efficiency [15], [16]. Support material can address these issues due to enhanced photocatalytic activity. Zeolite-supported photocatalyst materials have emerged as attractive photocatalysts due to their improved characteristics and potential applications in environmental remediation [17], [18]. Zeolites, with their high surface area and adsorption capacity, are good support materials for both TiO_2 and ZnO photocatalyst, increasing its photocatalytic efficacy [17]. This combination has been investigated for a variety of applications, including the degradation of contaminants and water treatment. Composites of TiO_2 and zeolite have higher photocatalytic activity than bare TiO_2. Supporting TiO_2 and ZnO particles on zeolite increases surface area and reduces agglomeration, leading to this improvement [17], [18], [19] [20]. Composites of TNZ and ZNZ have higher photocatalytic activity than bare TiO_2 and ZnO. The integration of TNZ and ZNZ in filtering systems can lead to the development of self-cleaning water treatment systems, enhancing sustainability and efficiency [21], [22].

Several studies have shown that irradiation period, photocatalyst mass, and sample concentration all have a substantial influence on the photodegradation process. These parameters are critical in defining the effectiveness and kinetics of photocatalytic degradation for a variety of contaminants and systems. In general, longer irradiation times accelerate degradation. For instance, under ideal conditions, full breakdown of metalaxyl was accomplished in under 30 minutes [23]. The mass of the photocatalyst is also critical; for example, a zinc oxide catalyst at 2.0 g/L yielded the maximum degradation rate of azo dyes, while greater doses decreased efficiency [24]. Similarly, the ideal loading of TiO_2/Fe_3O_4-SiO_2 was determined to be 0.962 g/L for maximal naphthalene degradation [25]. The concentration of the dye also influences degradation; for methyl orange, a concentration of 7 mg/100 mL resulted in 68% disintegration after 60 minutes [26]. Higher dye concentrations can decrease degradation effectiveness due to heightened competition for active sites on the photocatalyst [27].

This study synthesizes TNZ and ZNZ photocatalysts and determines their optimal performance in degrading CRD by adjusting irradiation length, photocatalyst mass, and dye concentration. The synthetic catalyst will be further investigated utilizing XRD (X-Ray Diffraction), FTIR (Fourier Transform Infrared), and UV-Vis DRS (Diffuse Reflectance Spectroscopy).

2. Materials and methods

2.1 Materials

The materials that used in this study were TiO_2 and ZnO (Sigma Aldrich), concentrated HCl, ethanol (96% pure), commercial Congo red dye and distilled water. Natural zeolite used was obtained from Bandung, West Java, Indonesia.

2.2 Preparation and activation of Natural Zeolite (NZ)

Natural zeolite preparation was carried out by weighing 150 grams of natural zeolite, which was then mashed and sieved through a 200 mesh. NZ was soaked in distilled water (1:2). This mixture was then mixed for 30 minutes before being filtered and dried in an oven set to 100°C for 2 hours. Furthermore, the solid was placed in a desiccator and weighed to ensure a constant weight.

A number of natural zeolites were immersed in concentrated chloride acid for 3 h before being activated by NZ. Following that, the solution was filtered and neutralized with distilled water. The NZ powder was dried for 2 h at 100°C and then calcined for 4 h at 500°C.

2.3 Synthesis of TNZ

The TNZ photocatalyst was created by mixing powder TiO_2 and activated natural zeolite (1:2), and then adding 48 mL of 96% ethanol. The TiO_2 and zeolite mixture was mixed with an agate mortar for an hour before being placed in a sonicator set to 24 kHz for 30 minutes. Next, the suspension was dried in an oven at 110°C for 3 h before being calcined at 500°C for 6 h. The solid was then milled into powder [28].

2.4 Synthesis of ZNZ

The ZNZ was prepared by combining activated natural zeolite with powder ZnO in a 2:1 ratio. Then, ethanol (98%) was added, and the mixture was stirred and heated with a heat and magnetic stirrer for 4 h. It was then oven dried for 5 h at 120°C before being calcined for 2 hours at 400°C [29].

2.5 Characterization of TNZ and ZNZ

Powder XRD measurements were performed on PANalytical X'Pert Pro for TiO_2 anatase, powder ZnO, NZ, TNZ and ZNZ using Cu-K radiation at 1.5418 Å. The optical band gap of the catalyst was determined using the Thermo Scientific Evolution 220 UV-Visible spectrophotometer and diffuse reflectance spectra (DRS). The sample reflectance ranged between 200 and 800 nm. FTIR measurements were performed using the Varian FT-1000 for determining the interaction on TNZ. In addition, the Varian Cary® UV-Visible spectrophotometer was used to evaluate the UV spectrums of both degraded and undegraded materials.

2.6 Photodegradation of CRD

In a 100 mL standard flask, 10 mg of CRD was diluted with distilled water to make a 100 ppm stock solution. The stock was reduced to a concentration of 10 ppm. In a beaker glass, 25 mL of 10 ppm CRD solution (pH 4-5) was mixed with 50 mg (TNZ) and in another beaker glass with 200 mg (ZNZ) of photocatalyst. The photodegradation of CRD was carried out under UV light for periods ranging from 20 to 120 minutes. Aliquots were collected and centrifuged to remove any

catalyst particles from the solution before being examined with a UV-Visible spectrophotometer at 497 nm wavelength. The same approach was used for TNZ photocatalyst masses ranging from 20 to 50 mg and ZNZ photocatalyst masses ranging from 50 to 250 mg, with the previously found optimum period. The optimum time and mass were then utilized to test different CRD concentrations (5-25 ppm).

3. Results and discussion

3.1 Characterization of TNZ and ZNZ

The materials were characterized using X-Ray Diffraction (XRD), UV-Visible Diffuse Reflectance Spectroscopy (DRS), and Fourier Transform Infrared (FTIR). Natural zeolite (NZ) and TiO_2 anatase precursors were studied, as well as TNZ and ZNZ composites. XRD and UV-Vis DRS were used to evaluate TiO_2, NZ, TNZ, and ZNZ. Meanwhile, TNZ was also evaluated using FTIR.

3.1.1 X-Ray Diffraction (XRD)

Diffraction shows that a TNZ (Figure 1a) and ZNZ (Figure 1c) composite was generated. The XRD pattern shows that there has been no chemical or structural change to NZ, since both TiO_2, ZnO and NZ peaks are evident. Furthermore, the absence of further peaks in TNZ and ZNZ suggests that the composite is free of contaminants. XRD examination showed that the TiO_2 phase formed during synthesis is anatase, whereas the zeolite phase is mordenite in TNZ, mordenite and clinoptilolite in ZNZ. Position shift caused by TNZ alteration and impregnation treatment. Increased particle size in TiO_2 and TNZ results in a shift to the right (Figure 1b).

Figure 1a displays the X-ray diffraction (XRD) patterns of NZ, TiO_2 anatase, TNZ, and their matching Joint Committee on Powder Diffraction Standards (JCPDS) references. The NZ sample shows typical peaks belonging to mordenite zeolite, which is consistent with the JCPDS reference for mordenite (JCPDS No. 06-0239) and confirms its crystalline form. TiO_2 anatase exhibits distinct peaks at $2\theta \approx 25.3°$, 37.8°, 48.0°, 53.9°, and 55.1°, corresponding to the (101), (004), (200), (105), and (211) planes, indicating the anatase phase of TiO_2 (JCPDS No. 21–1272). The preservation of the anatase phase indicates that the deposition procedure does not result in phase transformation to rutile, which is advantageous for photocatalytic applications due to anatase's higher activity. Figure 1b focuses on the major anatase (101) peak at around 25.3°. In comparison to pure anatase TiO_2, the TNZ composite peak is somewhat broader and shifts marginally. The broadening indicates decreased crystallite size or higher microstrain, while the shift may be attributed to lattice distortion caused by TiO_2 particles interacting with the zeolite surface or partial integration of Ti species into the zeolite framework.

Figure 1c depicts the XRD patterns of NZ, ZNZ, and the related JCPDS patterns of ZnO (JCPDS ZnO No. 36-1451), clinoptilolite zeolite standard (JCPDS No. 39-1383), and mordenite zeolite standard (JCPDS No. 06-0239). The NZ sample matches the diffraction peaks of clinoptilolite and mordenite, showing that the natural zeolite has a mixed-phase composition. The ZNZ composite has high peaks at $2\theta \approx 31.8°$, 34.4°, 36.3°, 47.5°, 56.6°, 62.9°, and 68.0°, which correspond to the hexagonal ZnO planes (100), (002), (101), (102), (110), (103), and (112). These peaks are consistent with the JCPDS card for ZnO, showing the effective integration of ZnO onto the zeolite.

Overall, the XRD results from Figures 1a-c demonstrate that both TNZ and ZNZ composites preserve their crystalline structure following production. These structural properties are believed to influence surface reactivity, light absorption, and, ultimately, the catalytic performance of composites.

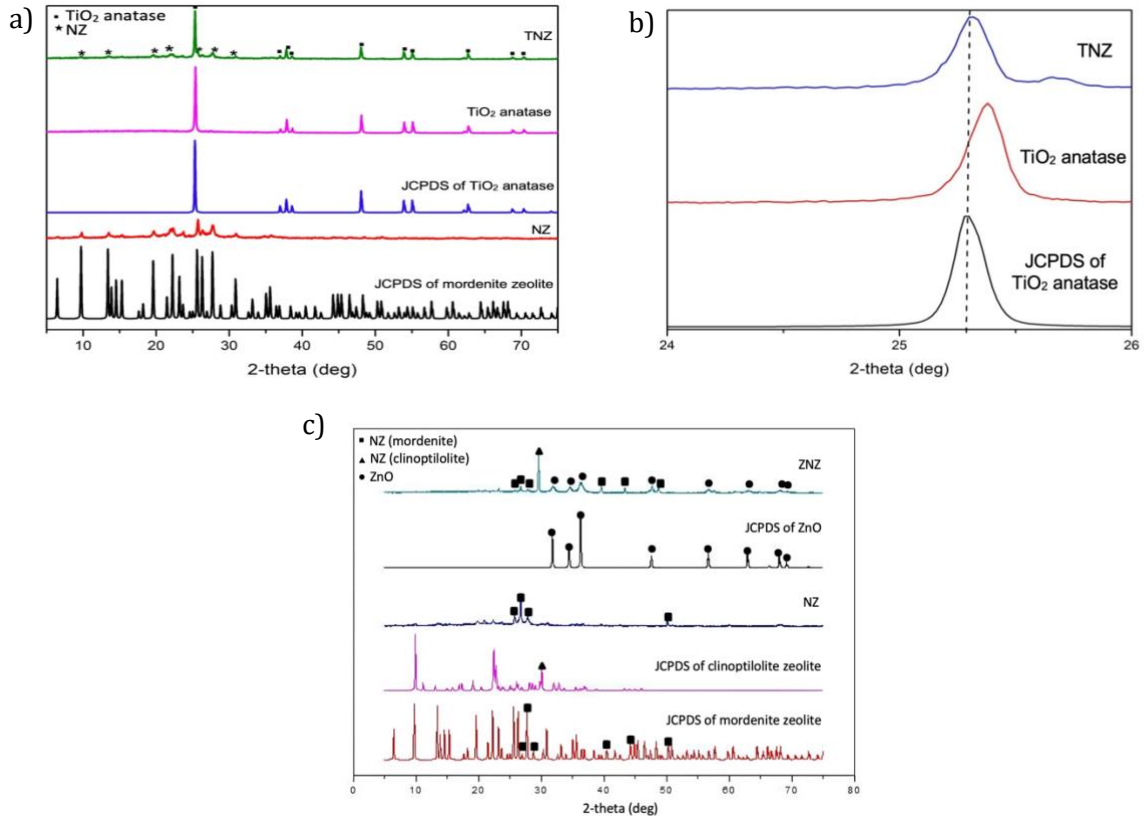

Figure 1. a) XRD plots of TNZ and comparison with commercial TiO_2 anatase, natural zeolite, standard TiO_2 (JCPDS No. 21-127) and mordenite zeolite standard (JCPDS No. 06-0239) samples; **b)** Enlargement of XRD plots of the TNZ, TiO_2 anatase and JCPDS of TiO_2; **c)** XRD plots of ZNZ and comparison with JCPDS of ZnO, natural zeolite, mordenite zeolite standard (JCPDS No. 06-0239) and clinoptilolite zeolite standard (JCPDS No. 39-1383).

3.1.2 UV-Visible Diffuse Reflectance Spectroscopy (DRS) and band gap energy analysis

The band gap energy (Eg) was determined using the Tauc plot method for indirect allowed transitions, where $(F(R)*h\nu)^{1/2}$ is plotted versus photon energy ($h\nu$) (Figure 2). TNZ photocatalyst has a lower band gap energy than pure TiO_2 (Figure 2a). Similarly, ZNZ photocatalyst exhibits the same tendency as TNZ (Figure 2b), these making it a better photocatalyst for photodegradation.

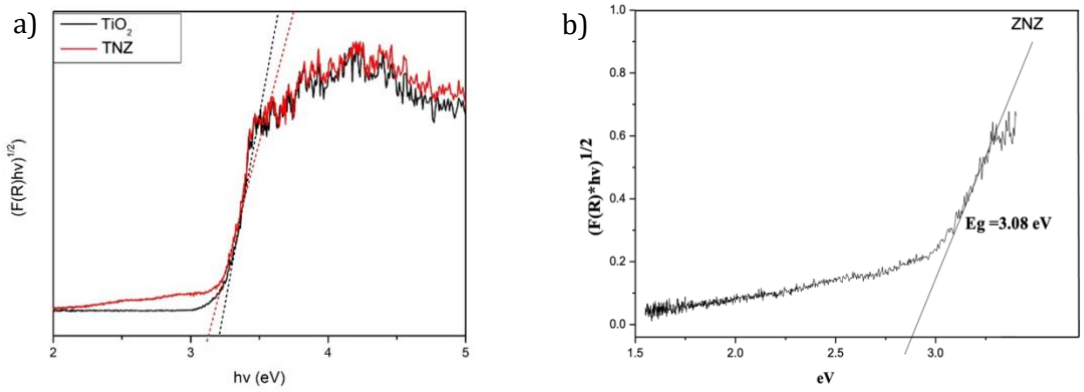

Figure 2. Tauc plot of **a)** TNZ and TiO_2 anatase; **b)** ZNZ; plotted using Kubelka- Munk function.

The TNZ has a slightly lower band gap energy of 3.12 eV than pure TiO_2 (3,20 eV). Similarly, the band gap energy's reference value for ZnO is 3.37 eV [30], [31], whereas ZNZ has a lower band gap of 3.08 eV. The interaction of ZnO particles with the zeolite framework may account for this change toward lower energy. Both modified photocatalyst, TNZ and ZNZ has a lower band gap energy than its unmodified form. The lowering of the band gap in both TNZ and ZNZ composites suggests that zeolite not only serves as a physical support but also changes the semiconductor's electrical structure. This alteration may encourage improved solar spectrum utilization and may boost photocatalytic efficiency under visible or near-visible light irradiation.

3.1.3 Fourier Transform Infrared (FTIR) spectroscopy

Figure 3 displays the FTIR data for TNZ, NZ and pure TiO_2. The anatase TiO_2 spectra show typical absorption peaks at wave numbers 3441 and 1634 cm^{-1}, corresponding to OH stretching and bending vibrations. The absorption of TiO_2 itself is represented by the Ti-O bending vibration at wave number 450 cm^{-1}. In the spectra of NZ, there are typical absorption peaks at wave numbers 3474 and 1645 cm^{-1} indicating OH stretching and bending vibrations, the asymmetric stretching vibration T-O-T (T:Si/Al) shown at 1054 cm^{-1}, 622-793 cm^{-1} is the symmetric stretching vibration T-O-T (Al-O-Al/O-Si-O), and 462 cm^{-1} is the bending vibration of Al-O or Si-O.

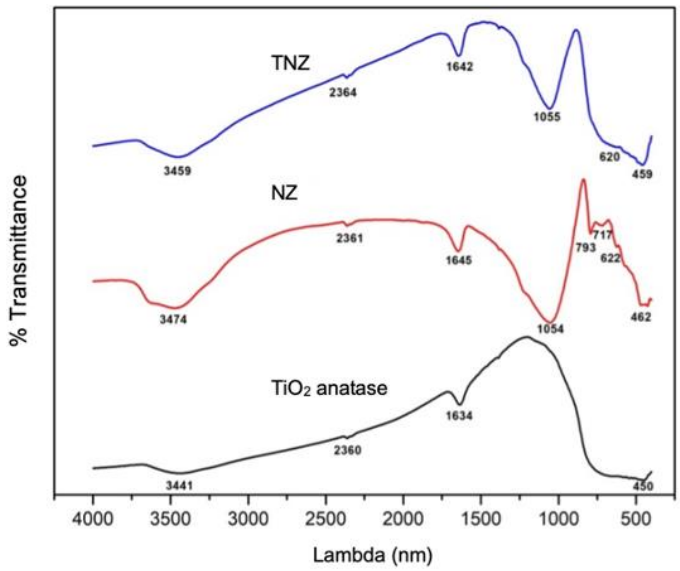

Figure 3. FTIR spectra of TNZ, NZ, and pure TiO_2.

Based on these results, TNZ exhibits a characteristic absorption peak at wave number 620 cm^{-1} (asymmetric stretching vibration O-Si-O/O-Al-O). In the absorption of this wave number, there is a peak broadening induced by overlapping or overlapping resulting from the absorption of 717 and 793 cm^{-1}, which are categorized as symmetric stretching vibration O-Si-O/O-Al-O and are therefore not evident in the TNZ spectra. According to previous research, wave numbers between 600-790 cm^{-1} show that TiO_2 interacts with the zeolite's outer pore system, resulting in the production of Ti-O-Si or Ti-O-Al bonds [32].

3.2 Photocatalysis

3.2.1 Effect of the irradiation time on the CRD degradation

Furthermore, five additional trials with stirring for 20, 40, 60, 80, 100, and 120 minutes were carried out to establish the best irradiation period for maximum CRD degradation. The photocatalyst mass and CRD concentration remained constant at 50 mg (TNZ)/25 mL solution, 200 mg (ZNZ)/25 mL solution and 10 ppm, respectively.

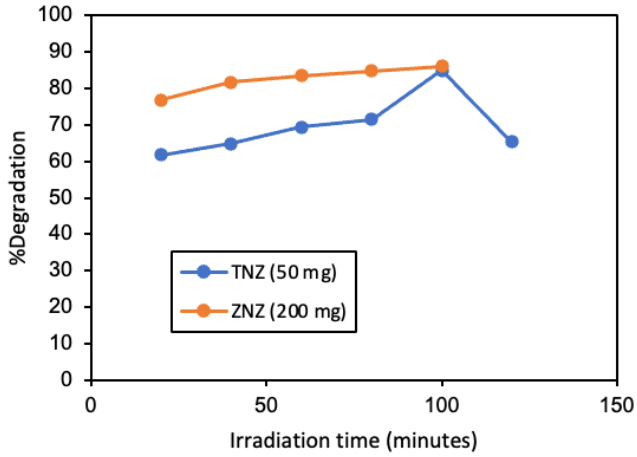

Figure 4. Degradation percentage of TNZ and ZNZ photocatalyst to degrade 10 ppm CRD in different irradiation time.

Figure 4 depicts the photocatalytic degradation efficiency of TNZ (50 mg) and ZNZ (200 mg) at different irradiation periods. Both catalysts showed an increase in degradation percentage with increasing irradiation time, up to an optimum point, after which a drop or plateau occurred. The percentage degradation of TNZ steadily rose from 61.8% at 20 minutes to 84.97% at 100 minutes. Beyond this point, deterioration efficiency dropped to 65.29% after 120 minutes. The first rise is attributed to the increasing creation of photoinduced electron-hole pairs, promoting the formation of reactive oxygen species (ROS) such as hydroxyl radicals (•OH) and superoxide anions (O_2•$^-$), responsible for pollutant breakdown. However, the drop after 100 minutes could be attributed to photocatalyst saturation and electron-hole pair recombination, which reduce ROS availability. Furthermore, extended irradiation may cause the build-up of intermediates on the catalyst surface, obstructing active sites and reducing light absorption.

On the other hand, ZNZ showed considerably greater photocatalytic activity over the course of all irradiation durations, rising from 76.80% at 20 minutes to 86.04% at 100 minutes. After 80 minutes, the performance plateau indicates that most of the target pollutant molecules had been broken down, and additional irradiation had no effect on efficiency. Due to its higher catalyst dosage (200 mg), which offers a larger surface area and more active sites for photocatalytic reactions.

3.2.2 Effect of the photocatalyst mass on the CRD degradation

Figure 5 shows how photocatalyst mass affects degradation percentage (%) for both TNZ and ZNZ photocatalysts. At 50 mg catalyst loading, TNZ had the maximum degradation percentage of 96.78%. The degradation percentage gradually decreased with additional catalyst mass, reaching

87.51% at 150 mg. This decrease can be due to increasing turbidity in the suspension with larger catalyst loadings, which inhibits light penetration and consequently restricts the production of reactive species on the photocatalyst surface. Furthermore, too many catalyst particles may encourage agglomeration, which would reduce the amount of effective surface area that is accessible for photocatalytic processes.

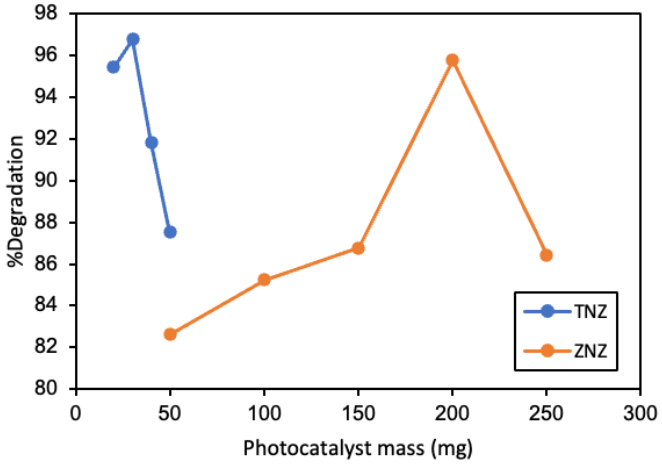

Figure 5. Degradation percentage of TNZ and ZNZ photocatalyst to degrade 10 ppm CRD with mass variation of photocatalyst at optimum irradiation time.

On the other hand, ZNZ showed a distinct trend, with degradation efficiency increasing from 82.62% at 50 mg to 95.76% at 200 mg. This improvement shows that, for ZNZ, a greater catalyst mass gives more active sites while not significantly reducing light penetration up to 200 mg. However, at 250 mg, the efficiency dropped to 86.43%, showing that above the optimal loading, the same light scattering and agglomeration effects occurred as with TNZ. The difference in optimal catalyst mass between TNZ (50 mg) and ZNZ (200 mg) might be attributed to crystallinity, as revealed by XRD examination. TNZ, with better crystallinity and perhaps smaller crystallite size, has more active sites per unit mass and hence reaches peak performance at lower loadings. In contrast, ZNZ may have bigger crystallite sizes or lower surface reactivity, necessitating the use of more material to provide an adequate number of active sites for efficient degradation.

3.2.3 Effect of initial CRD concentration on the degradation

The influence of initial CRD concentration on photocatalytic degradation percentage using TNZ (30 mg) and ZNZ (200 mg) photocatalysts is presented in Figure 6. The degrading percentage of TNZ increased from 75.05% at 5 ppm to a peak of 96.78% at 10 ppm, then gradually decreased to 83.68% at 25 ppm. A similar trend was seen for ZNZ, with the highest degrading percentage (97.32%) at 15 ppm, followed by a little fall to 94.80% at 20 ppm and 83.68% at 25 ppm.

The first rise in degradation percentage as CRD concentration increases up to the optimal point can be due to increased dye molecule availability, which improves photon absorption and accelerates photocatalytic processes on the catalyst surface. However, above the optimal concentration, the degradation efficiency declined. This decrease can be attributed to the excessive accumulation of dye molecules on the catalyst surface, which can block active sites and prevent light penetration into the suspension. Furthermore, high dye concentrations can result in

an inner filter effect, in which incident photons are absorbed by dye molecules before reaching the photocatalyst surface, decreasing the formation of reactive species such hydroxyl radicals (•OH).

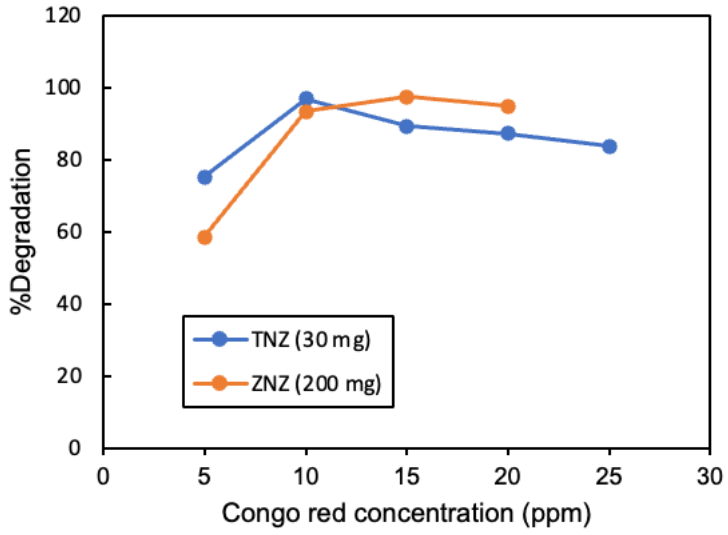

Figure 6. Degradation percentage of TNZ and ZNZ photocatalyst to degrade CRD at different concentrations at optimum irradiation time and photocatalyst mass.

Interestingly, ZNZ exhibited lower degradation efficiency than TNZ at low concentrations (5–10 ppm), but surpassed TNZ performance at moderate concentrations (15–20 ppm). This difference suggests that the higher mass loading of ZNZ (200 mg) provides more available active sites, which becomes advantageous when more dye molecules are present in the solution. At low concentrations, however, the excess catalyst mass may cause light scattering or shielding effects, leading to suboptimal photon utilization.

4. Conclusion

The optimal irradiation time for TNZ and ZNZ photocatalyst to decompose CRD is 100 minutes, the optimal mass of TNZ and ZNZ photocatalyst for decomposing CRD was 30 mg and 200 mg per 25 mL, respectively. Meanwhile, TNZ can degrade CRD at optimal concentration 10 ppm, ZNZ at 15 ppm, the best resulting in a maximum above 95% degradation rate for both TNZ and ZNZ but at lower mass of TNZ.

References

[1] Lukman J 2023 *The Jakarta Post* Accessed: Aug. 03, 2025 [Online]
[2] Rani E G, Rao M V L N R, Sundary M B T, Chandra B R and Kiran C H R 2013 *IOSR J. Comput. Eng.* **14** 50–54
[3] Siddiqui S I, Allehyani E S, Al-Harbi S A, Hasan Z, Abomuti M A, Rajor H K and Oh S 2023 *Processes* **11** 807
[4] Hernández-Zamora M, Martínez-Jerónimo F, Cristiani-Urbina E and Cañizares-Villanueva R O 2016 *Ecotoxicology* **25** 1832–1840
[5] Quintanilla-Villanueva G E, Sicardi-Segade A, Luna-Moreno D, Núñez-Salas R E, Villarreal-Chiu J F and Rodríguez-Delgado M M 2025 *Catalysts*, **15** 84
[6] Lugo-Ruiz A A and Bailón-Ruiz S J 2024 *Photochem* **4** 222–232
[7] Liang R, Hatat-Fraile M, He H, Arlos M, Servos M R and Zhou Y N 2017 *Proc. of SPIE* **9545** 95450M

[8] Latuheru P M, Utami F D, Sari Y P, Sulistiyono N, Rahmayanti H D, Rahman D Y, Maemunah I R 2024 *Jakarta International Conference on Multidisciplinary Studies towards Creative Industries* (JICOMS) *KnE Eng.* 662-667
[9] Setyarsih W, Rohmawati L, Ardiansyah F F M, Maarif S and Darminto D 2025 *Trends Sci.* **22** 2-11
[10] Abisha P, C G Jinitha and Sonia S 2024 *Curr. Appl. Phys.* **60** 79–91
[11] Hamdan A M, Azkiya R, Rahman A, Efriana M, Maulana R and Hanif H 2023 *J. Fis. Dan Apl.* **19** 11-16
[12] Bhapkar A R and Bhame S 2024 *J. Environ. Chem. Eng.* **12** 112553
[13] Porley V and Robertson N 2020 *Nanostructured Photocatalysts* 129–171
[14] Puri N and Gupta A 2023 *Environ. Res.* **227** 115786
[15] Pan L, Shen G, Zhang J, Wei X, Wang L, Zou J and Zhang X 2015 *Ind. Eng. Chem. Res.* **54** 7226–7232
[16] Yang B, Ma Z, Wang Q, and Yang J 2022 *Catalysts* **12** 268
[17] Mergenbayeva S, Abitayev Z, Batyrbayeva M, Vakros J and Poulopoulos S G 2022 *IOP Conf. Ser. Earth Environ. Sci.* **1123** 012086
[18] Huayna G, Laura A, Churata R, Lazo L, Guzman R, Ramos P G and Rodriguez J M 2023 *Appl. Sci.* **14** 3146
[19] Aini N, Chasanah S N, Khalifah S N, Arifah A, Prasetyo A, and Suendo V 2019 *IOP Conf. Ser. Mater. Sci. Eng.* **622** 012006
[20] Munguti L K, Dejene F B and Muthee D K 2023 *Mater. Chem. Phys.* **295** 127063
[21] Manea F and Orha C 2019 *Photocatalysts - Applications and Attributes 99-114*
[22] Diantariani N P, I Kartini, Kuncaka A and Wahyuni E T 2020 *Rasayan J. Chem.* **13** 747–756
[23] Islam J B, Furukawa M, Tateishi I, Katsumata H and Kaneco S 2020 *SN Appl. Sci.* **2** 925
[24] Effiong J F, Nyong A E, Boekom E J and Simon N 2023 *Asian J. Appl. Chem. Res.* **13** 23–32
[25] Zhou A, Peng J, Chen Z, Du J, Guo Z, Ren N and Wang A 2012 *Int. J. Photoenergy* **2012** 1–9
[26] Rahman M, Pinky T A, Mondal D C, Abedin M and Hasan M 2020 *J. Mater. Sci. Res. Rev.* **5** 1-14
[27] Singh G, Ubhi M K, Jeet K, Singla C and Kaur M 2023 *Processes* **11** 1727
[28] Sene R A, Moradi G R, and Sharifnia S 2017 *Ultrason. Sonochem.* **37** 490–501
[29] Darajat S, Aziz H and Alif A 2015 *J. Ris. Kim.* **1** 179
[30] Baskoutas S 2018 *Materials* **11** 873
[31] Hassan N K and Hashim M R 2012 *International Conference on Enabling Science and Nanotechnology* 1–2
[32] Rahman A, Nurjayadi M, Wartilah R, Kusrini E, Prasetyanto E A and Degermenci V 2018 *Int. J. Technol.* **9** 1159